

Cite this: *RSC Sustainability*, 2026, 4, 1964

# Production of syringic acid by direct CO<sub>2</sub> insertion into syringol *via* a Kolbe–Schmitt type reaction

Omar Mohammad, <sup>a</sup> Jude A. Onwudili <sup>\*ab</sup> and Qingchun Yuan <sup>ab</sup>

Syringic acid (4-hydroxy-3,5-dimethoxybenzoic acid) is a valuable hydroxybenzoic acid with applications in pharmaceuticals, food additives, and polymeric materials such as poly(phenylene oxide) (PPO). Despite its industrial relevance, current synthesis methods are reported only in patents, relying on expensive precursors such as syringaldehyde and multi-step chemical reactions, leading to high production costs and chemical waste. In contrast, syringol, a biomass-derived phenolic compound, is commercially available at half the cost of syringaldehyde, making it a more economical alternative. This study presents, for the first time, a one-pot method for the direct carboxylation of syringol to produce syringic acid. Initial experiments using sodium syringolate (SyONa) and the conventional Kolbe–Schmitt reaction yielded only 0.53% syringic acid. However, at 225 °C and *p*CO<sub>2</sub> between 5 and 50 bar over 2–6 hours, the addition of guaiacol or potassium carbonate (K<sub>2</sub>CO<sub>3</sub>) significantly promoted the yield of syringic acid. Guaiacol enhanced conversion but led to substantial by-product formation, whereas K<sub>2</sub>CO<sub>3</sub> improved selectivity to syringic acid (up to 90%) and increased the yield to 39.2% after 6 h. A mechanistic analysis indicates that K<sub>2</sub>CO<sub>3</sub> activates the *para*-C–H bond of syringolate more effectively than guaiacol, enabling a previously inaccessible carboxylation pathway. By leveraging CO<sub>2</sub> as a reactant and biomass-derived feedstock, this work aligns with Green Chemistry principles, reducing reliance on costly reagents and minimising chemical waste. These findings not only offer a sustainable route for syringic acid synthesis but also open new possibilities for the large-scale production of green PPO, advancing the development of bio-based polymers for a sustainable future.

Received 1st April 2025  
Accepted 26th February 2026

DOI: 10.1039/d5su00232j

rsc.li/rscsus

## Sustainability spotlight

The study demonstrates that CO<sub>2</sub> can be used as a feedstock to produce syringic acid *via* the Kolbe–Schmitt carboxylation of bio-derived syringol, achieving up to 39% molar yield. This offers a more sustainable route to a compound that is otherwise difficult to obtain. Promoters such as potassium carbonate and guaiacol improved performance: potassium carbonate increased product purity, while guaiacol generated additional useful carboxylated side products. The method reduces processing steps and waste compared with conventional biochemical or extractive production routes, supporting greener manufacturing. Our results highlight the potential for scaling CO<sub>2</sub> utilisation to produce high-value organic chemicals, which aligns with UN SDGs on industry and innovation (SDG 9), responsible production (SDG 12), and climate action (SDG 13).

## Introduction

Syringic acid (4-hydroxy-3,5-dimethoxybenzoic acid) is a naturally occurring hydroxybenzoic acid with applications in pharmaceuticals, food additives, and biobased materials due to its antioxidant, antimicrobial, and anti-inflammatory properties.<sup>1</sup> It serves as a key building block in the synthesis of bioactive compounds, dyes, and polymeric materials such as poly(phenylene oxide) (PPO), which is widely used as a high-performance engineering plastic due to its high thermal and chemical resistance.<sup>2</sup> Oxidative degradation of syringol-rich

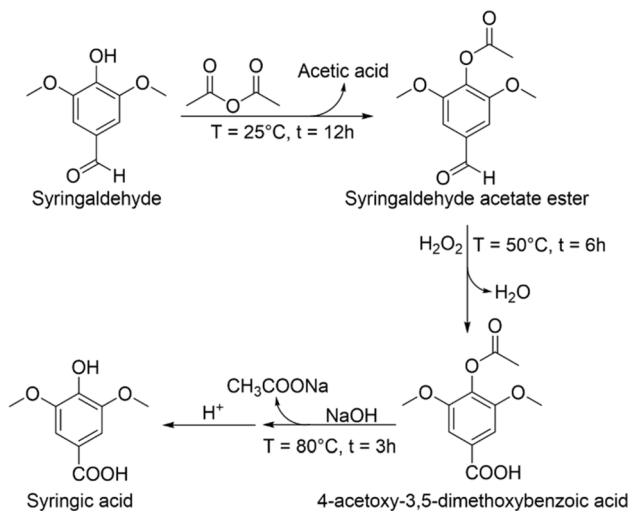
lignin or microbial fermentation methods often suffer from low yields and complex purification steps.<sup>3</sup> As a result, syringic acid has been predominantly produced through chemical and biocatalytic routes or extracted from natural resources.<sup>4–6</sup> Notably, while no detailed chemical synthesis routes have been reported in scientific research articles, they are described in patents,<sup>4–6</sup> highlighting their industrial relevance but limited academic exploration.

For instance, the reported chemical routes for syringic acid synthesis include methods starting from syringaldehyde (4-hydroxy-3,5-dimethoxybenzaldehyde). The syringaldehyde-based method involves three main steps as shown in Scheme 1: first, esterification of syringaldehyde with acetic anhydride to form syringaldehyde acetate ester (4-acetoxy-3,5-dimethoxybenzaldehyde); second, oxidation of this ester using hydrogen peroxide to yield 4-acetoxy-3,5-dimethoxybenzoic

<sup>a</sup>Energy and Bioproducts Research Institute, Aston University, Aston Street, Birmingham, West Midlands, B4 7ET, UK. E-mail: j.onwudili@aston.ac.uk

<sup>b</sup>Department of Chemical Engineering and Biotechnologies, Aston University, Aston Street, Birmingham, West Midlands, B4 7ET, UK





**Scheme 1** Schematic synthesis of syringic acid from syringaldehyde (4-hydroxy-3,5-dimethoxybenzaldehyde), involving three steps: (1) esterification with acetic anhydride, (2) oxidation with hydrogen peroxide, and (3) hydrolysis.<sup>4</sup>

acid; and finally, hydrolysis of the oxidised ester to produce syringic acid (yield = 86.5% and purity = 98.6%).<sup>4</sup> In the latter chemical route, 3,4,5-trimethoxybenzoic acid undergoes selective demethylation by treatment with a hydrogen bromide solution in glacial acetic acid. This reaction removes one of the methoxy groups ( $-\text{OCH}_3$ ) from the aromatic ring, converting it into a hydroxyl group ( $-\text{OH}$ ) to form syringic acid. The patent reported a syringic acid yield of 85.3%. While the purity of the product was not stated, the formation of minor side products, such as small amounts of polyhydroxy benzoic acid, was noted. Further purification was achieved through crystallisation from the highly water-soluble side products.<sup>7</sup>

The biocatalytic route involves utilising microbial cells, such as *E. coli*, to convert shikimic acid into syringic acid through an enzymatic cascade. The process employs enzymes such as shikimate kinase, chorismate lyase, mutant hydroxylases, and *o*-methyltransferases to catalyse the sequential modifications of shikimic acid, resulting in the formation of syringic acid. While minor by-products are produced, the final product would require further purification and extraction by crystallisation to achieve high purity.<sup>6</sup>

Additionally, the extraction of syringic acid from natural sources, such as plant biomass, has been reported in a patent.<sup>5</sup> For example, oat biomass is known to contain between 0.46 and 1.8% by mass of syringic acid, which can be obtained by a process involving multi-step extraction. This process begins with supercritical  $\text{CO}_2$  fluid extraction, carried out at temperatures of 40–50 °C and pressures of 200–300 bar over 1–3 hours, allowing extraction of syringic acid along with other phenolic compounds. The crude extract is then purified through column chromatography using silica gel or resin, which separates syringic acid from impurities in a process lasting 2–4 hours, depending on column parameters. The final purification step involves crystallisation, where the compound is dissolved in ethanol or a similar solvent and cooled over 12–24 hours to yield a highly pure product with over 98%

purity. This method achieved a yield of 8.4 g of syringic acid from 1 kg of oat biomass, representing an efficiency of 60–75% based on syringic acid content.<sup>5</sup>

As discussed, the industrial method uses syringaldehyde as the starting material, requiring three separate steps with additional chemical reagents. This process generates chemical waste and extends production time to approximately 21 hours. Furthermore, syringol is commercially available at half the cost of syringaldehyde, making this new approach more economical and viable. Direct carboxylation of syringol is a promising alternative primarily derived from lignocellulosic biomass, particularly hardwoods and herbaceous plants, which are rich in syringyl lignin.<sup>8</sup> Biomass sources such as poplar and miscanthus contain high syringyl-to-guaiacyl ratios, making them promising feedstocks for syringol production.<sup>9</sup> Among the limited methods available, the Kolbe–Schmitt reaction is the only direct process for the insertion of  $\text{CO}_2$  into an aromatic C–H bond.<sup>10</sup> However, this reaction is only effective for compounds that have at least one unoccupied *ortho*-position relative to the hydroxyl ( $-\text{OH}$ ) group for  $\text{CO}_2$  insertion. In the case of syringol, both *ortho*-positions are occupied by methoxy ( $-\text{OCH}_3$ ) groups, leaving the *para*-position as the only potential site for carboxylation. However, because of its electrophilicity,  $\text{CO}_2$  preferentially inserts at the position of the highest electron density on the aromatic ring. This occurs at the *ortho*-position due to the closer proximity and delocalisation of the lone pair of electrons from the hydroxyl group into the aromatic ring.<sup>11</sup> Hence, *para*-carboxylation is not thermodynamically favoured.

If successful, this method would offer the dual advantage of potentially utilising eco-friendlier, biomass-derived syringol while incorporating the most ubiquitous greenhouse gas,  $\text{CO}_2$ , directly into the process to produce syringic acid under moderate reaction conditions. Although there are no available data for the current global production volume of syringic acid, market analysis indicates that the syringic acid market is projected to experience a compound annual growth rate (CAGR) of over 6.5% between 2024 and 2030.<sup>12</sup> This growth is driven by the versatile applications of syringic acid across various industries, including pharmaceuticals (such as the production of the methylphenidate prodrug),<sup>13</sup> cosmetics and food and beverage industries, where it functions as a natural sweetener.<sup>14</sup>

Previously, among the native phenolic compounds (*e.g.* phenol, 2-cresol and catechol) guaiacol improved the yield of syringic acid from sodium syringolate the most without undergoing extensive carboxylation itself.<sup>15</sup> Further tests showed that using pre-formed phenolate salts, *e.g.*, sodium 2-methoxyphenolate, led to significant formation of 3-methoxy-salicylic acid, vanillic acid, and 2,4-dicarboxy-6-methoxyphenol, which reduced overall selectivity towards syringic acid.<sup>15</sup>  $\text{K}_2\text{CO}_3$  was selected because Marasse reported its ability to promote *para*-carboxylation,<sup>16</sup> and it avoids introducing any additional organic species, ensuring that no new intermediates for carboxylation are generated. The chosen promoter loading (50 wt%) and reaction temperature were based on previous optimisation work on a carboxylation mixture of five different phenolics,<sup>15,17</sup> where the yield of syringic acid increased from 4.84% at 175 °C to 31.2% and 33.0% at 200 °C and 225 °C,



respectively, with no further benefit at higher promoter concentrations.

This study presents a series of novel experiments aimed at addressing the limitations of traditional industrial synthesis for syringic acid. The objective of this work is to demonstrate that direct CO<sub>2</sub> insertion into an aromatic C–H bond of syringol is achievable using guaiacol and a combination of different alkali metals, enabling the one-pot synthesis of high-purity syringic acid. Experiments were conducted at 225 °C, with reaction time and pressure systematically varied to investigate their effects on syringic acid yield. Obtaining appreciable yields of syringic acid from this work may offer a sustainable pathway to produce this high-value chemical from renewable biomass and abundant CO<sub>2</sub> under moderate reaction conditions.

## Materials and methods

### Materials

The chemicals used in this study for the preparation of sodium syringolate were syringol (HO(CH<sub>3</sub>O)<sub>2</sub>C<sub>6</sub>H<sub>3</sub>, 154.16 g mol<sup>-1</sup>, 99% purity) and sodium hydroxide (NaOH, 98.5% purity). Syringol was also formed as a reaction product and was used in the external calibration method. The corresponding hydroxybenzoic acid products were also purchased for quantification using the external standard method, which included syringic acid (HO(CH<sub>3</sub>O)<sub>2</sub>C<sub>6</sub>H<sub>2</sub>COOH, 97% purity), 3-methoxysalicylic acid (CH<sub>3</sub>OC<sub>6</sub>H<sub>3</sub>(OH)COOH, 97% purity), vanillic acid (HOC<sub>6</sub>H<sub>3</sub>(OCH<sub>3</sub>)COOH, 98% purity), and 2,3-dihydroxyterephthalic acid ((HO)<sub>2</sub>C<sub>6</sub>H<sub>2</sub>(COOH)<sub>2</sub>, 97% purity). Guaiacol (C<sub>6</sub>H<sub>4</sub>(-OH)(OCH<sub>3</sub>), >99% purity) and potassium carbonate (K<sub>2</sub>CO<sub>3</sub>, 99% purity) were used as promoters in the reaction. Toluene (C<sub>6</sub>H<sub>5</sub>CH<sub>3</sub>, HPLC grade, 99.85% purity) was employed to wash the solid product post-reaction, while acetone ((CH<sub>3</sub>)<sub>2</sub>CO, HPLC grade, 99.8% purity), formic acid (99% purity), and methanol ((CH<sub>3</sub>OH) HPLC grade, 99% purity) were used as solvents for sample work-up and analysis. All chemical reagents and solvents were obtained from Fisher Scientific (Leicester, UK). Carbon dioxide (industrial grade, 99.8% purity) was supplied in a 6.5 kg portable cylinder by BOC Gases, UK. Deionised water, used for sample preparation for HPLC analysis, was obtained in-house *via* a Q-pod system.

### Preparation of sodium syringolate

The sodium salt of syringol (SyONa) was synthesised according to Kolbe's method.<sup>10,18</sup> Initially, one mole of syringol was dissolved in an equimolar solution of sodium hydroxide (NaOH). To ensure complete dissolution of NaOH, it was first dissolved in water at three times its weight before the addition of syringol. Excess water was critical, as the immediate interaction of syringol with NaOH produced solids that could impede stirring. Therefore, excess water was added to maintain proper stirring throughout the reaction and to prevent solidification for a homogeneous mixing. The resulting mixture was loaded into a glass-lined 450 mL 4575A fixed-head bench-top Parr reactor vessel equipped with a stirrer. The reaction was carried out at 130 °C for 4 hours at a stirring rate of 50 rpm. Following the

reaction, the reactor was cooled to 40 °C, as cooling below this temperature caused solidification of the salts, complicating their recovery. The phenolic salt solution was transferred to a beaker and dried in a vacuum oven at 40 °C overnight. The dried SyONa was then removed, crushed to a particle size of 125–250 μm, and stored in an air-tight container for further use.

### Purity characterisation of sodium syringolate (SyONa)

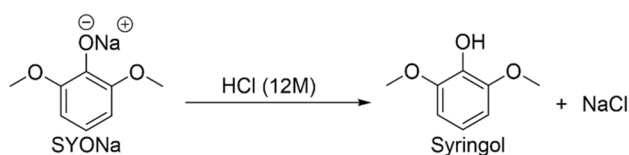
A new method for testing the purity of sodium salts of phenolics was developed and detailed in our previous work.<sup>17</sup> The purity of sodium syringolate (SyONa) was determined through gravimetric analysis of NaCl, verified *via* back-acidification. Approximately 1 g of SyONa was acidified by adding droplets of 12 M HCl, resulting in the formation of syringol and NaCl (Scheme 2). The mixture was dried to remove excess water, and acetone was used to extract the syringol, leaving behind white crystals of NaCl. The acetone was filtered using a Büchner funnel, with the NaCl solids retained on the filter paper, while the acetone-syringol solution passed through. The NaCl recovery was calculated as the ratio of the obtained NaCl mass to the theoretical NaCl mass, multiplied by 100. The recovery was 98.0%, demonstrating high purity of SyONa.

The second technique involved quantifying syringol post-acidification. A known mass of SyONa was first dried in a vacuum oven and then acidified in a 10 mL vial using droplets of concentrated HCl (12 M). The remaining volume was filled with a 50% v/v water–acetone solution to ensure complete dissolution of both syringol and NaCl. The resulting solution was analysed using High-Performance Liquid Chromatography (HPLC). A calibration curve for syringol in water–acetone (50% v/v) was prepared, achieving an *R*-squared value of 0.998. Using this calibration curve, the average syringol recovery over three replicates was calculated to be 96.8 ± 3.22. The minor discrepancy in mass was attributed to moisture or trace impurities. These results confirm that highly pure SyONa was used, ensuring an accurate mass balance for subsequent reactions.

The HPLC method employed for syringol quantification was the same as described in a previous work<sup>17</sup> and used for characterising all other hydroxybenzoic acids (HBAs). The recovery of both syringol and NaCl indicated excellent mass balance, validating the purity of the SyONa for further reactions.

### Carboxylation of the sodium salt of syringol (SyONa) *via* the Kolbe–Schmitt reaction using guaiacol and K<sub>2</sub>CO<sub>3</sub> as promoters

The conventional Kolbe–Schmitt reactions were conducted in a set of 4 × 10 mL Quadracell reactors supplied by Asynt



Scheme 2 Acidification of the sodium salt of syringol (SyONa) to produce syringol and NaCl.



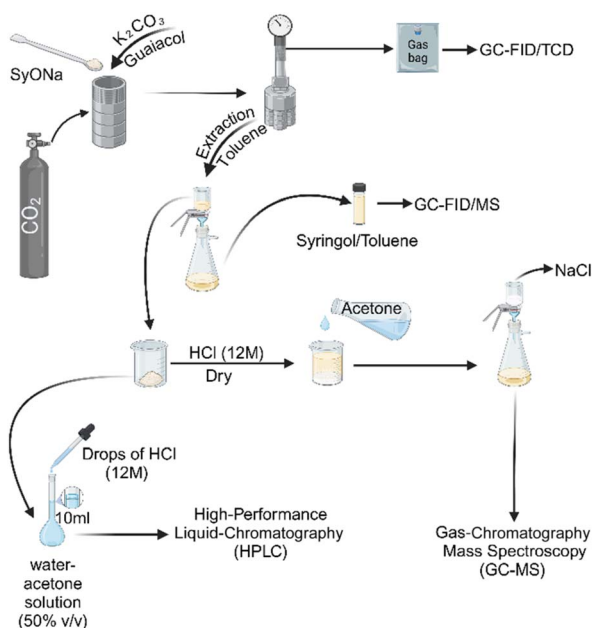
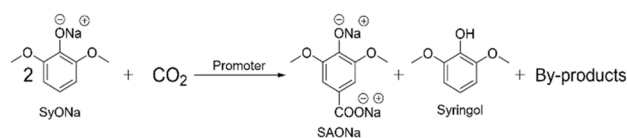


Fig. 1 The overall methodology for carboxylation of the sodium salt of syringol (SyONa) with addition of guaiacol and  $K_2CO_3$  as promoters (created using BioRender. Mohammad, O. (2025) <https://BioRender.com/f28k370>).

(Isleham, Cambridgeshire, United Kingdom) as detailed in a previous report.<sup>19</sup> In each reactor cell, a measured mass of SyONa (0.3 g) was added. The reaction promoters, guaiacol and  $K_2CO_3$  were then added into the mixture using 50 wt% of the initial mass of SyONa (0.15 g). All four reactor cells were then sealed onto the main reactor cap and purged with  $CO_2$  to remove any residual air. The reactor system was pressurised to the target operating pressure (5 bar, 10 bar, 30 bar and 50 bar) using a two-stage piston cylinder regulator (GASARC, Tech Master GPT420 Series). The regulator valve controlled the maximum delivery pressure, and a digital pressure transducer monitored the pressure. The reactor was weighed before and after  $CO_2$  pressurisation to determine the exact mass of  $CO_2$  introduced and the average standard deviation between them was  $\pm 0.06$  g. The reactors were heated to 225 °C, at a rate of 10 °C  $min^{-1}$ . The reaction mixture was maintained at the target temperature for set times (2, 4 and 6 hours) before being allowed to cool to room temperature. Reaction temperatures were controlled using an Asynt ADS-HP-NT magnetic stirrer hotplate, and pressure readings were displayed *via* a digital pressure gauge integrated with a cooling tower. The overall methodology for the carboxylation of SyONa for syringic acid production is summarised in Fig. 1.

### Characterisation of the syringol/toluene mixture by gas-chromatography flame ionisation detection and mass spectroscopy (GC-FID/MS)

Based on the work conducted in the previous report,<sup>17</sup> the carboxylation reaction of phenolics would yield approximately one mole each of the sodium salt of hydroxybenzoic acids (HBAs) and precursor phenolic compound. An example with



Scheme 3 General reaction scheme showing the carboxylation of the sodium salt of syringol (SyONa) to form one mole of the sodium salt of syringic acid (SAONa) and one mole of syringol. The independent promoters used in this study were guaiacol and  $K_2CO_3$ .

syringol is shown in Scheme 3. In this present work, non-syringic acid products were recovered by washing the carboxylated products with approximately 50 mL of toluene and quantified using gas-chromatography flame ionisation detection (GC-FID). A calibration curve of syringol in toluene was constructed to quantify the mass of syringol formed during the reaction using an external standard *via* GC-FID. The GC-FID method was the same as the previously reported method.<sup>19</sup>

For qualitative analysis of other potential toluene-soluble organics and post-acidification products of SAONa, a Shimadzu gas chromatography-mass spectrometer (GC-MS, QP2010 SE) was used. The instrument was equipped with an SH-Rxi™-5ms capillary column (diphenyl dimethyl polysiloxane, 30 m length, 0.25 mm inner diameter, 0.25  $\mu m$  film thickness). The analysis conditions included a 1 : 20 split ratio and an initial temperature of 40 °C held for 5 minutes, followed by a ramp of 5 °C  $min^{-1}$  to 300 °C, which was held for 10 minutes. The injector temperature was set to 300 °C. A quadrupole mass detector with electron ionisation (operating relative to tuning results) was employed to detect ions within the range of 20–300  $m/z$ .

### Quantification of carboxylation products of sodium syringolate (SyONa) using high-performance liquid chromatography (HPLC)

A high-performance liquid chromatography (HPLC) method was developed in the previous work to characterise the HBA products of the Kolbe–Schmitt reaction.<sup>17</sup> The carboxylation products of SyONa using  $K_2CO_3$  yielded mainly syringic acid with minor impurities. In contrast, using guaiacol as a promoter resulted in the formation of other products, such as 3-methoxysalicylic acid (3-MSA), vanillic acid (VA), and 2,4-dicarboxylic acid-6-methoxyphenol (2,4-DCA-6-MXP), due to substitution reactions between SyONa and guaiacol.

The quantification of syringic acid, 3-MSA, VA, and 2,4-DCA-6-MXP was carried out using calibration curves prepared from commercially available standards of these compounds at known concentrations. The standards were dissolved in a water–acetone solution (50% v/v), and calibration curves with *R*-squared values of 0.999 were achieved for all compounds. The HPLC method employed a reverse-phase Kinetex 5  $\mu m$  C18 100 Å, 250 × 4.6 mm column (Phenomenex Ltd, UK) with a mobile phase consisting of water with 0.1% formic acid (Solvent A) and methanol (Solvent B). The gradient program was as follows: 5.0 min (90% A, 10% B), 20.0 min (70% A, 30% B), 30.0 min (50% A, 50% B), and 40.0 min (30% A, 70% B). The flow rate was kept at 0.5 mL  $min^{-1}$ , with an injection volume of 10  $\mu L$ .



Detection was performed using a UV detector set at 254 nm with a bandwidth of 4 nm at a column temperature of 30 °C. The retention times of the reaction products matched those of the commercially available standards. For the commercially unavailable 2,4-DCA-6-MXP, quantification was performed using 2,3-dihydroxyterephthalic acid as a calibration standard. Additionally, the calibration curve of syringol was constructed to quantify the unreacted syringol.

### Calculating the yield and conversion of syringic acid

The molar yields of syringic acid were calculated based on the initial amount of SyONa (0.3 g) added to each reactor based on a 1 : 1 molar ratio. The first step involved determining the moles of SyONa fed to the reactor. The next step involved determining the moles of syringic acid from the HPLC data using its peak area and calibration curve. A similar approach was applied to quantify the unreacted syringol. The syringol formed during the reaction was recovered using toluene and quantified by constructing a calibration curve for syringol in a toluene solution using GC-FID. The molar yield of each product was calculated relative to the initial moles of SyONa using eqn (1).

$$\text{Molar yield(\%)} = \frac{n_{\text{Product}}}{n_{\text{SyONa}_{\text{fed}}}} \times 100 \quad (1)$$

Here, the moles of products ( $n_{\text{Product}}$ ) correspond to syringic acid and syringol (from the toluene fraction).

The conversion was calculated as the ratio of unreacted moles of SyONa ( $n_{\text{SyONa}_{\text{unreacted}}}$ ) to the initial moles ( $n_{\text{SyONa}_{\text{fed}}}$ ), expressed as a percentage as shown in eqn (2).

$$\begin{aligned} \text{Conversion(\%)} &= 1 - \left( \frac{n_{\text{SyONa}_{\text{unreacted}}}}{n_{\text{SyONa}_{\text{fed}}}} \right) \times 100 \\ &= \frac{\sum \text{products}}{n_{\text{SyONa}_{\text{fed}}}} \times 100 \end{aligned} \quad (2)$$

Finally, validation of this method was conducted through ensuring the total moles for all products ( $\sum_n \text{products}$ ) and unreacted SyONa ( $n_{\text{SyONa}_{\text{unreacted}}}$ ) accounted for the initial amount of SyONa fed to the reactor ( $n_{\text{SyONa}_{\text{fed}}}$ ). An example is shown in eqn (3).

$$n_{\text{Syringic acid}} + n_{\text{Syringol}_{\text{toluene}}} + n_{\text{SyONa}_{\text{unreacted}}} \cong n_{\text{SyONa}_{\text{fed}}} \quad (3)$$

Additionally, the molar yields of products deemed to have formed from guaiacol (see above) as a promoter were determined using the same methodology; however, their yields were calculated relative to the initial mass of guaiacol added (0.15 g).

## Results and discussion

### Effect of pressure on syringic acid yield and by-product formation using guaiacol or $\text{K}_2\text{CO}_3$ as a promoter

The novelty of this work is the first demonstration that  $\text{CO}_2$  can be inserted directly into syringol (*via* sodium syringolate),

despite both *ortho*-positions being blocked, by enabling a promoter-assisted *para*-carboxylation route under Kolbe-Schmitt-type conditions. This is not a routine substrate extension, because syringolate cannot undergo the conventional *ortho*-carboxylation pathway; instead, promoter choice governs whether *para*-carboxylation is accessible and whether side reactions dominate.

The feasibility of using syringol obtained directly from lignin depolymerisation as a feedstock has also been explored. However, lignin depolymerisation does not yield pure phenolics; it produces complex mixtures containing numerous aromatic and non-phenolic compounds.<sup>20</sup> When these crude mixtures were converted into their sodium salts and subjected to Kolbe-Schmitt carboxylation, no detectable carboxylated products were formed. This indicated that a certain level of isolation of lignin-derived phenolics would be required in future work. A recent study has shown that addition of phenol to sodium phenoxide can promote the reaction significantly.<sup>17</sup> In this work, adding syringol to sodium syringolate did not enhance syringic acid formation, yielding only 0.53%. However, it was discovered that guaiacol as a promoter can aid in promoting syringic acid formation.<sup>15</sup> Therefore, guaiacol was selected for further optimisation, with experiments conducted at reaction times of 2, 4, and 6 hours and varying  $\text{CO}_2$  pressures of 5, 10, 30, and 50 bar. The only limiting factor was the continued formation of significant amounts of by-products, including 3-methoxysalicylic acid (3-MSA), vanillic acid (VA), and a dicarboxylic acid derivative of guaiacol. This by-product revealed that hydroxybenzoic acid (HBA) production can occur through an *in-situ* sodium-proton exchange mechanism.<sup>21</sup> In this work, SyONa reacted with guaiacol by transferring a sodium ion to form sodium guaiacolate, which then underwent carboxylation. This process generated a mixture of HBAs. Fig. 2(a) illustrates the product distribution from the carboxylation of SyONa with guaiacol as a promoter *via* HPLC. Since the efficiency of the process depends on minimising by-product formation, an alternative strategy has to be explored to enhance selectivity and yield.

To address this challenge, various carbonate salts were tested, revealing that a mixture of potassium carbonate ( $\text{K}_2\text{CO}_3$ ) and

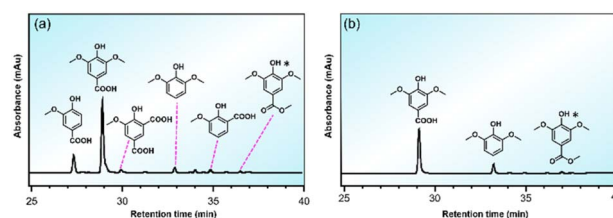
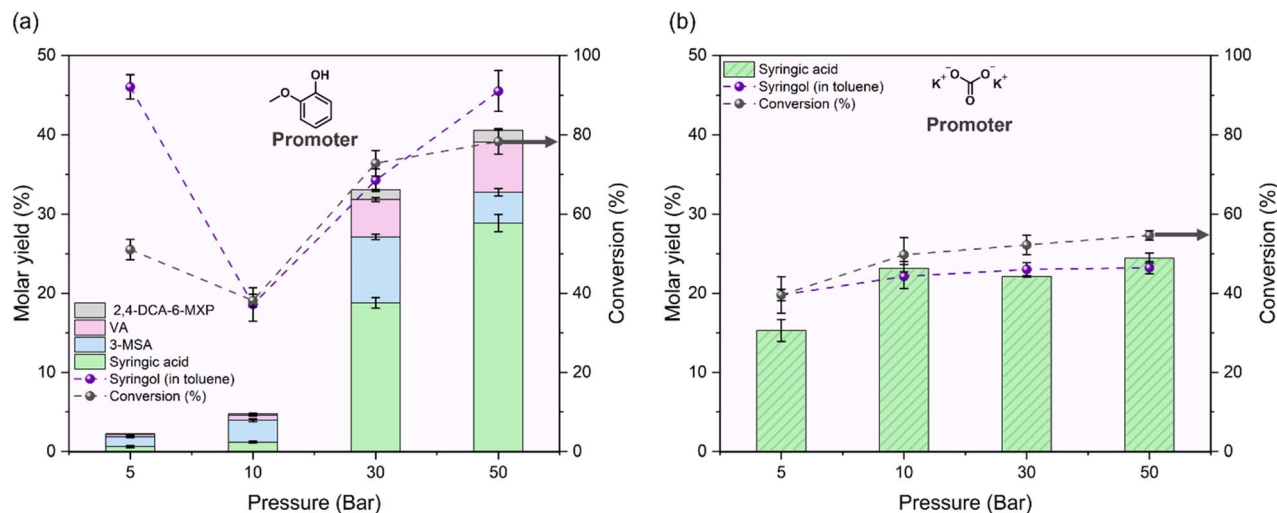


Fig. 2 Comparative HPLC chromatograms illustrating product distributions from the carboxylation of sodium syringolate (SyONa) under different promoters: (a) reaction with guaiacol as a promoter, yielding syringic acid along with a wide range of hydroxybenzoic acid (HBA) by-products derived from guaiacol, and (b) reaction using potassium carbonate ( $\text{K}_2\text{CO}_3$ ) as a promoter, which produced primarily syringic acid with only minor formation of methyl syringate (marked with an asterisk \*). The methyl syringate was confirmed as the sole product in the solid fraction *via* GC-MS analysis.





**Fig. 3** Results of the carboxylation of sodium syringolate (SyONa) under two different conditions: (a) with guaiacol as a promoter and (b) with potassium carbonate ( $K_2CO_3$ ) as a promoter. For each experiment, 0.15 g of the promoter was added to 0.3 g of SyONa under reaction conditions of ( $T = 225\text{ }^\circ\text{C}$ ,  $t = 2\text{ h}$ , and  $pCO_2 = 5\text{--}50\text{ bar}$ ). The molar yield of syringic acid was calculated based on a 1 : 1 molar ratio relative to the initial mass of SyONa, while the molar yield of guaiacol-derived products was calculated based on the 0.15 g of guaiacol added.

sodium syringolate (SyONa) effectively promoted syringic acid formation while significantly reducing by-products, as shown in Fig. 2(b). Based on this finding, a comparative optimisation study was carried out using both guaiacol and  $K_2CO_3$  as reaction promoters. The results of the carboxylation of SyONa using guaiacol as a promoter shown in Fig. 3(a) demonstrate an increasing trend in syringic acid formation with rising  $CO_2$  pressure. The syringic acid yield increased from 0.61% at 5 bar, to 1.18% at 10 bar to 18.8% at 30 bar and 28.9% at 50 bar. Similarly, the conversion of SyONa also improved with pressure, as the formation of syringol increased from 18.6% at 10 bar to 34.3% and 45.5% at 30 bar and 50 bar, respectively. However, the conversion was higher at 5 bar, with a higher formation of sodium guaiacolate, indicating lower pressure increases the rate of sodium-proton exchange, as less  $CO_2$  is available to facilitate the reaction, leaving the sodium syringolate susceptible to sodium-proton exchange. The increases in conversion and syringol formation were attributed to sodium-proton exchange between SyONa and guaiacol. The formation of HBA products derived from guaiacol, namely 3-MSA, VA, and 2,3-DCA-6-MXP, also increased with pressure, rising from 1.63% at 5 bar to 3.57% at 10 bar and to 14.3% at 30 bar, before slightly decreasing to 11.7% at 50 bar. Notably, other impurities, including various guaiacol and syringol derivatives, were detected both in the toluene fraction and the final solid products. As shown in Table S1, these compounds likely formed through substitution reactions involving the methoxy groups of phenolics and hydroxyl groups. In the toluene fraction, the by-products accounted for less than 7.5% of the normalised peak areas, with 1,2,3-trimethoxybenzene (1,2,3-TMB) being the most prominent. In the solid fraction, methyl syringate (0.31–0.52%) and 1,2-benzenediol-3-methoxy or 3-methoxycatechol (3-MC) (0.22–1.31%) were the main impurities, although their values remained relatively low. It is noteworthy that many of the aforementioned by-products were below the detection limit at 5 bar.

For the carboxylation of SyONa using 50 wt%  $K_2CO_3$  relative to the initial mass of SyONa, the effect of pressure was not as significant beyond 10 bar as shown in Fig. 3(b). The yield of syringic acid at 5 bar was 15.3%. However, the yield remained relatively unchanged at 23.2% at 10 bar, 22.1% at 30 bar, and 24.4% at 50 bar. The yield of syringol in the toluene fraction showed a slight increase from 19.8% at 5 bar, to 22.1%, 23.0% and 23.2% at 10, 30, and 50 bar, respectively. This suggested that the reaction followed a 2 : 1 molar ratio, where for every two moles of SyONa, approximately one mole of syringic acid and one mole of syringol were formed (Scheme 3).

Earlier studies by Kolbe<sup>22</sup> showed similar trends, when reacting sodium phenoxide in an open system. The issue of phenol volatilisation was mitigated by increasing the pressure in a closed system, which helped to shift the equilibrium from disodium salicylate formation towards mono-sodium salicylate, thereby regenerating sodium phenoxide for further reaction cycles. This led to the achievement of an overall 1 : 1 molar ratio of salicylic acid from sodium phenoxide.

The GC-MS spectra of the toluene fractions for reactions with guaiacol and  $K_2CO_3$  as promoters are shown in Fig. 4(a) and (b), respectively. Similarly, the solid fractions for the two promoters are presented in Fig. 4(c) and (d). For comparison, Fig. 4(a) shows a greater variety of side products, including derivatives from both syringol and guaiacol derivatives. These by-products likely resulted from methyl group substitution reactions between syringol, guaiacol, and their respective HBAs. In contrast, Fig. 4(b) shows a simpler product profile since syringol was the only compound present.

Here, the formation of 1,2,3-TMB can be attributed to a reaction between two syringol molecules, yielding both 1,2,3-TMB and 3-MC, followed by further substitution reactions. It is noteworthy that 1,2,3-TMB was also detected in the pure syringol sample during GC-MS analysis, albeit in trace amounts



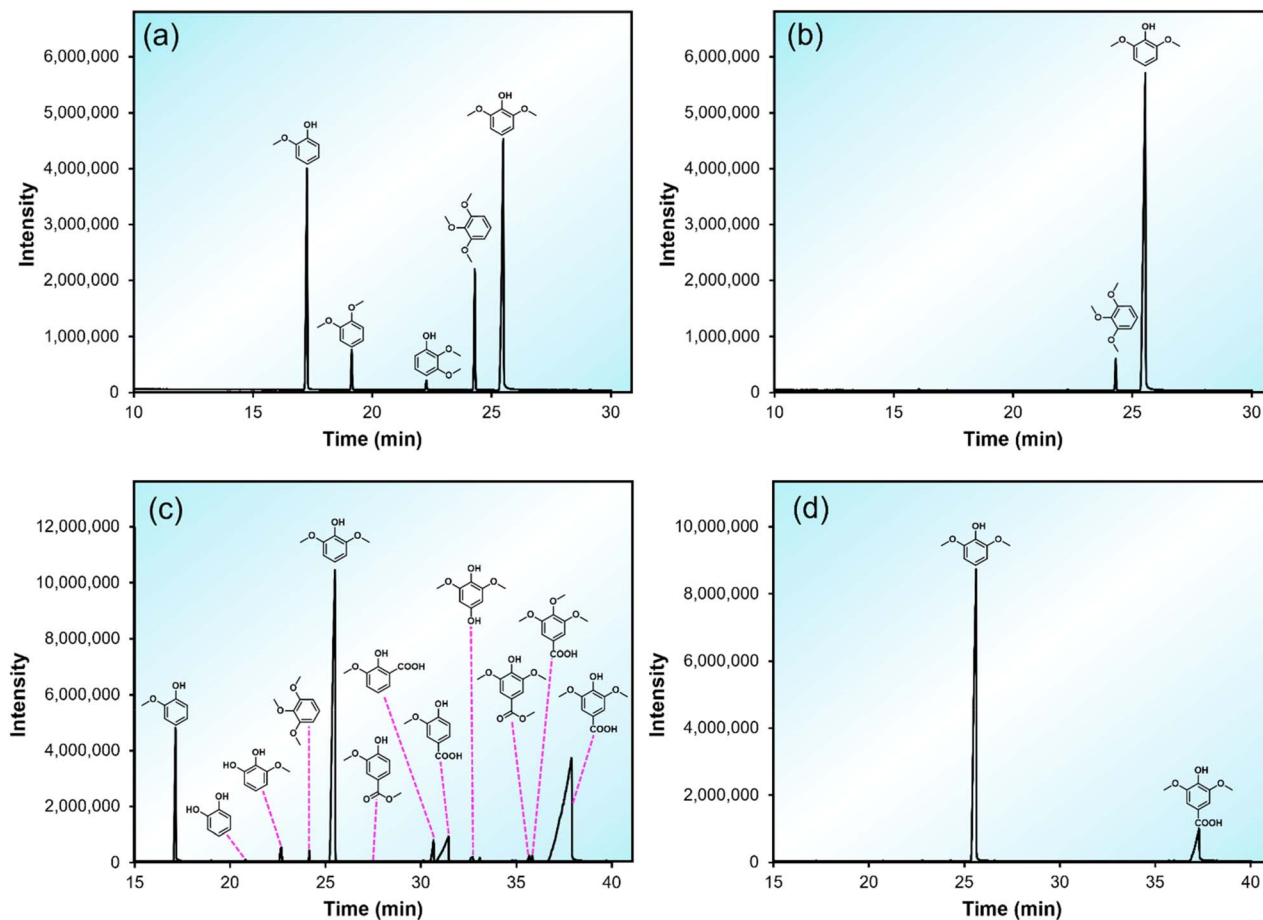


Fig. 4 GC-MS spectra illustrating the product distribution from the carboxylation of SyONa with different promoters at  $p\text{CO}_2 = 30$  bar: (a) toluene fraction from the reaction with guaiacol, showing a wide variety of syringol and guaiacol derivative by-products; (b) toluene fraction from the reaction with  $\text{K}_2\text{CO}_3$ , showing fewer by-products with 1,2,3-trimethoxybenzene (1,2,3-TMB) as a notable compound; (c) solid fraction from the reaction with guaiacol, indicating minor peaks of methyl syringate and other organics; and (d) solid fraction from the reaction with  $\text{K}_2\text{CO}_3$ , where only unreacted syringol and syringic acid were prominent, with trace amounts of methyl syringate.

(0.09%). It seems that the reaction has accelerated its formation.

The normalised peak areas of 1,2,3-TMB in the toluene fraction were 4.53% at 5 bar, 5.47% at 10 bar, 6.68% at 30 bar, and 4.85% at 50 bar, indicating that its concentration did not significantly change with increasing pressure. In the solid fraction obtained with  $\text{K}_2\text{CO}_3$  as the promoter (Fig. 4(d)), the most prominent peaks correspond to unreacted syringol and syringic acid. Along the chromatographic line, minor peaks are present, indicating trace amounts of other organic compounds. These peaks are not visually distinct due to their small intensity. Among the detected compounds, methyl syringate and 3-MC were the most notable, albeit in negligible quantities, with normalised peak areas ranging from below the detection limit to 0.34% for methyl syringate and up to 0.95% for 3-MC (Table S2).

#### Effect of reaction time on syringic acid yield and by-product formation using guaiacol or $\text{K}_2\text{CO}_3$ as a promoter

From previous studies on the effect of reaction time in the conventional Kolbe–Schmitt carboxylation of phenol, it was found that near-complete conversion occurs within 1 hour

producing approximately one mole each of phenol and salicylic acid.<sup>17</sup> However, with extended reaction time, phenol begins to react with disodium salicylate, forming mono-sodium salicylate and regenerating sodium phenoxide to sustain further reaction cycles. A similar trend was expected for the carboxylation of SyONa. However, as shown in Fig. 5(a), the yield of syringic acid did not increase after 6 hours of reaction time when guaiacol was used as a promoter. The conversion of SyONa into syringic acid reached 18.8% after 2 hours, 32.5% after 4 hours, and 27.8% after 6 hours. The trend showed an initial increase in conversion before plateauing at 6 hours. The conversion of SyONa correlated with an increased formation of syringol, which accounted for 34.3%, 36.3%, and 38.8% at 2, 4, and 6 hours, respectively. It was hypothesised that, as the reaction progressed, guaiacol underwent proton substitution with sodium from SyONa, effectively extracting sodium from syringol to facilitate carboxylation. The increased presence of guaiacol in the solid products suggests that upon acidification, the sodium salt reverted to guaiacol. These products would probably have remained in the organic toluene fraction had they not interacted with sodium during the reaction.



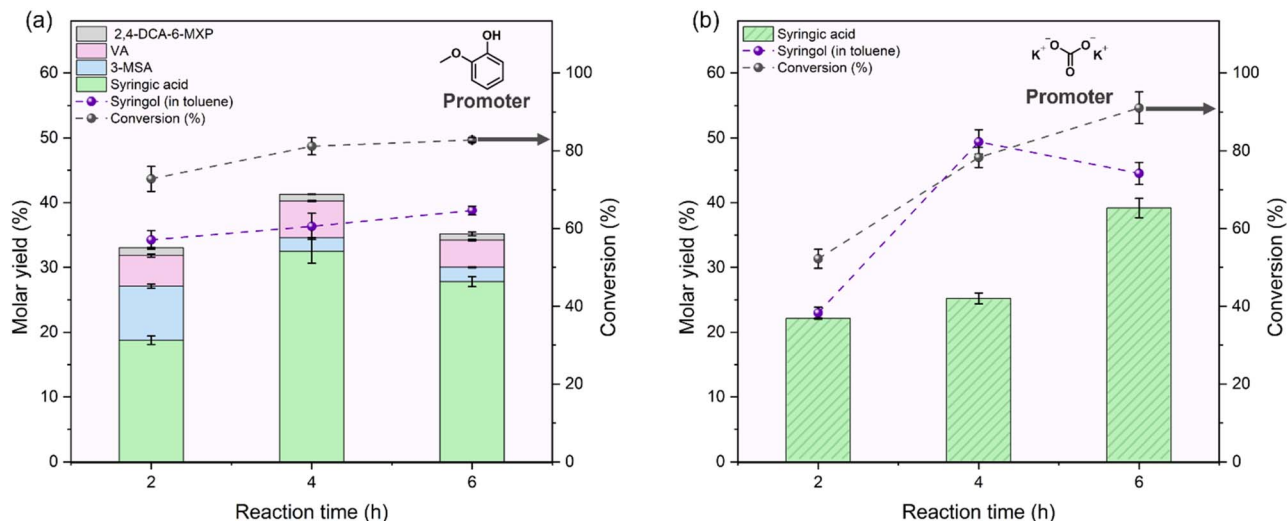


Fig. 5 Effect of reaction time on carboxylation of the sodium salt of syringol (SyONa) under two different conditions: (a) with guaiacol as a promoter and (b) with potassium carbonate (K<sub>2</sub>CO<sub>3</sub>) as a promoter. For each experiment, 0.15 g of the promoter was added to 0.3 g of SyONa under reaction conditions of  $T = 225\text{ }^{\circ}\text{C}$ ,  $p\text{CO}_2 = 30\text{ bar}$  and  $t = 2\text{ h}$ ,  $4\text{ h}$ , and  $6\text{ h}$ . The molar yield of syringic acid was calculated based on a 1 : 1 molar ratio relative to the initial mass of SyONa, while the molar yield of guaiacol-derived products was calculated based on the 0.15 g of guaiacol added.

The yields of HBA products derived from guaiacol decreased over time, from 14.3% at 2 hours to 8.82% at 4 hours and 7.34% at 6 hours. GC-MS analysis revealed increased formation of 1,2,3-trimethoxybenzene (1,2,3-TMB), which rose from 6.35% at 2 hours to 7.05% at 4 hours and 14.2% at 6 hours. Similarly, the relative abundance of 1,2-dimethoxybenzene changed from 2.81% to 2.15% and then to 4.23% over the same period (Table S3). These results indicated that syringol and guaiacol progressively lost protons, forming additional methoxy groups as the reaction time increased. The absence of syringol in later stages likely reduced the yield of syringic acid, as syringol could no longer regenerate and participate in further reaction cycles.

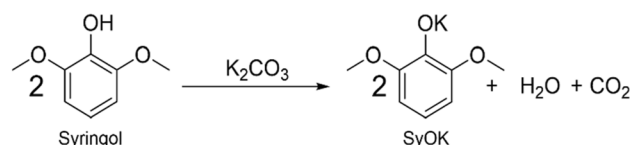
A different trend was observed when using K<sub>2</sub>CO<sub>3</sub> as the promoter (Fig. 5(b)), where the yield of syringic acid was 22.1% after 2 hours, 25.2% after 4 hours, and 39.2% after 6 hours. An increasing trend in conversion with reaction time was observed. The conversion of SyONa was maximal at 6 hours, reaching 91.0%, associated with the formation of syringol, whose yield increased from 23.0% at 2 hours to 49.4% at 4 hours, followed by a slight drop to 44.5% at 6 hours. It was plausible that, as the reaction proceeded, the *in-situ* produced free syringol was deprotonated to form potassium syringolate (SyOK), which participated in the reaction; however, this also resulted in water formation. The presence of water likely inhibited further reaction.<sup>18</sup> A schematic diagram of this reaction is presented in Scheme 4.

These results were consistent with the GC-MS analysis, which showed that at 6 hours, the formation of syringic acid was significantly higher, 85.4%. Common side products, such as 3-MC formation, exhibited normalised peak areas of 0.95% at 2 hours, 1.01% at 4 hours, and 1.35% at 6 hours. Methyl syringate formation also increased from 0.34% at 2 hours to 0.35% at 4 hours and 0.96% at 6 hours. Although the side reactions increased with time, the increase was not substantial, as they

were still at around 1%. In the toluene fraction, 1,2,3-TMB showed a rising trend, with peak areas of 6.68% at 2 hours, 12.2% at 4 hours, and 14.63% at 6 hours. This increase correlates with the formation of methyl syringate in the solid fraction, suggesting that as the reaction time progresses, a methyl group from syringol transfers to syringic acid, forming methyl syringate and 3-MC. Notably, 3-MC, containing two hydroxyl groups, can coordinate with two alkali metal species, potentially restricting further reaction. These preliminary findings are promising, as side product formation is inevitable even in industrial processes. The key advantage of this process is that it is a one-pot method and the only approach proposed for direct CO<sub>2</sub> insertion into the C–H bond of syringol to form syringic acid.

#### Proposed mechanism for the activation of sodium syringolate (SyONa) with guaiacol or K<sub>2</sub>CO<sub>3</sub> as a promoter

The Kolbe–Schmitt reaction of phenol, as the simplest model compound, has been investigated in detail by both density functional theory (DFT) calculations and experimental studies.<sup>17,23,24</sup> These studies provide a basis for formulating mechanisms for more substituted phenolic compounds. Accordingly, the mechanism proposed for the carboxylation of sodium syringolate follows analogous steps, with the first stage involving the formation of the SyONa–CO<sub>2</sub> complex (a), an



Scheme 4 Deprotonation syringol with K<sub>2</sub>CO<sub>3</sub> to form potassium syringolate (SyOK), accompanied by water formation.



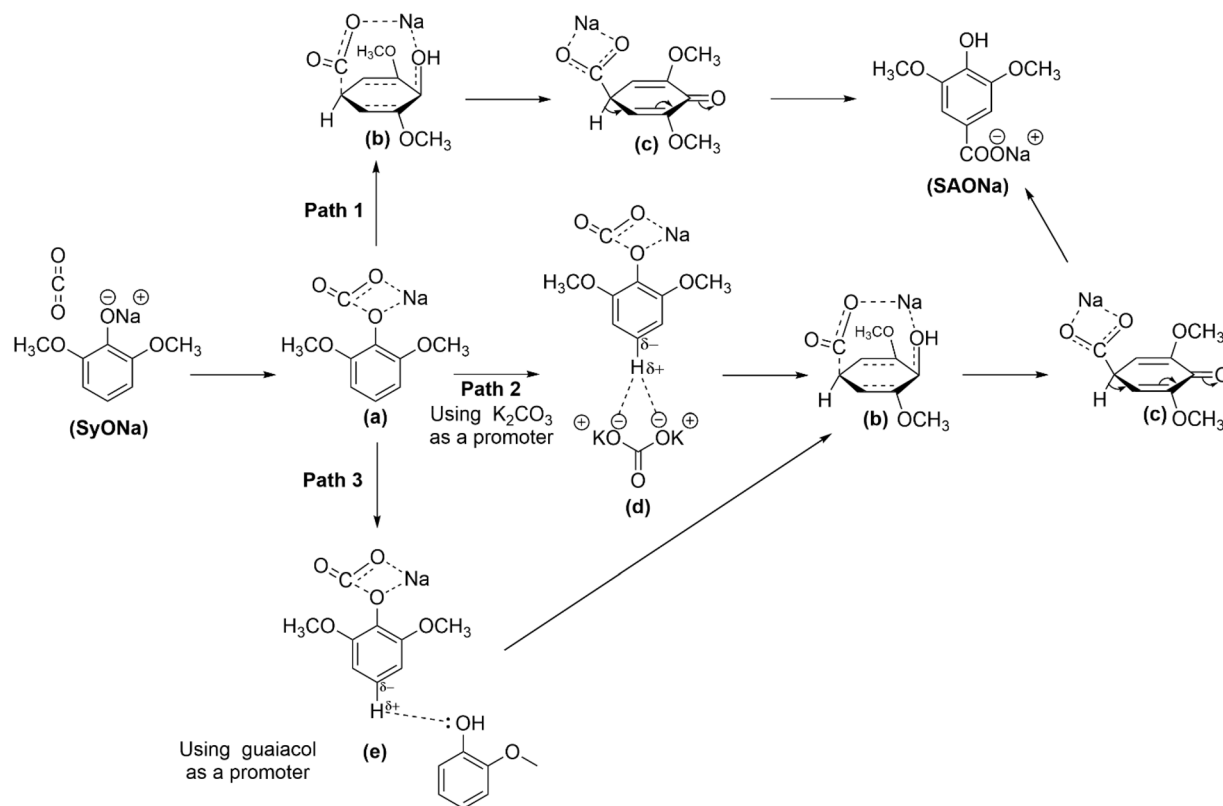


Fig. 6 Proposed pathways for the carboxylation of sodium syringolate. Path 1: the initial SyONa–CO<sub>2</sub> complex (a) proceeds through intermediates (b) and (c) to sodium syringate (SAONa), but this direct route is intrinsically unfavourable because both *ortho* positions are blocked by methoxy groups and the geometry between the phenoxide oxygen and the *para*-C–H bond does not readily allow a cyclic transition state. Path 2: with K<sub>2</sub>CO<sub>3</sub> as a promoter, complex (d) forms via a bifurcated O···H–C interaction that activates the *para*-C–H bond and promotes conversion through (b) and (c) to SAONa. Path 3: with guaiacol as a promoter, complex (e) forms via a weaker monodentate O···H–C interaction, resulting in only limited activation before conversion through (b) and (c) to SAONa.

intermediate that is widely accepted in the Kolbe–Schmitt reaction.<sup>17,24,25</sup> In the case of syringolate, however, both *ortho*-positions are occupied by methoxy groups, so the conventional *ortho*-carboxylation pathway available to phenol is sterically blocked. Under these constraints, the reaction is considered to proceed exclusively *via* the formation of complex (b), as shown in Fig. 6.

The direct conversion of the SyONa–CO<sub>2</sub> complex (a) into complex (b) is intrinsically disfavoured due to the distance and geometry between the phenoxide oxygen and the *para*-C–H bond, which do not readily permit a cyclic transition state. For phenol, the Kolbe–Schmitt reaction predominantly forms 2-hydroxybenzoic acid (2-HBA), since two *ortho*-positions (C-2 and C-6) and only one *para*-position (C-4) are available for carboxylation, giving a two-to-one statistical advantage to *ortho*-substitution.<sup>15</sup> In addition, resonance from the phenoxide increases electron density at the *ortho*-sites, and intramolecular hydrogen bonding in the transition states stabilises the *ortho* pathway relative to *para* pathway, as shown in previous mechanistic and DFT studies on sodium and potassium phenoxides.<sup>15,24,25</sup> In syringolate, by contrast, both *ortho*-positions are blocked by methoxy substituents, preventing the usual *ortho*-directed carboxylation and making a direct intramolecular approach of CO<sub>2</sub> to the *para*-position less favourable.

In the presence of K<sub>2</sub>CO<sub>3</sub>, complex (d) offers a way to overcome this intrinsic disadvantage. The two carbonate oxyanions can engage in a bifurcated O···H–C interaction with the *para*-C–H bond,<sup>26</sup> pre-organising the ion pair and polarising the C–H bond in a position that is more conducive to C–H activation. This behaviour is consistent with recent studies on carboxylate-assisted C–H activation in supported alkali carbonates, where dispersed M<sub>2</sub>CO<sub>3</sub> (M = K or Cs) promoted C–H deprotonation and CO<sub>2</sub> incorporation through a cyclic, carboxylate-stabilised transition state.<sup>26,27</sup> These systems demonstrate that carbonate bases can organise and polarise aromatic C–H bonds sufficiently to enable carboxylation under mild conditions. As shown in Fig. 6, guaiacol can also promote C–H activation through an O···H–C intermolecular bond between its phenoxide oxygen and the *para*-C–H bond in the SyONa–CO<sub>2</sub> complex (complex (e)).<sup>28</sup> However, this interaction is monodentate, involving only a single hydrogen-bond acceptor.<sup>29</sup> Methoxy-substituted phenols such as guaiacol are known to form relatively weak and easily disrupted hydrogen bonds due to intramolecular interaction,<sup>28</sup> providing far less geometric stabilisation than the bifurcated interaction observed with K<sub>2</sub>CO<sub>3</sub>. Consequently, the monodentate contact offered by guaiacol leads to only limited C–H activation, which is consistent with the lower selectivity and increased formation of side



products observed under guaiacol-promoted conditions. Rather than facilitating effective C–H activation, guaiacol primarily participates in sodium–proton exchange with SyONa, a phenomenon reported in earlier studies.<sup>15,21</sup>

## Conclusions

This work reports the first direct CO<sub>2</sub> insertion into the C–H bond of syringol to form syringic acid through the Kolbe–Schmitt reaction using guaiacol and K<sub>2</sub>CO<sub>3</sub> as promoters.

Under optimal reaction conditions in this work (225 °C, 4 hours, and 30 bar CO<sub>2</sub>), the use of guaiacol as a promoter increased the molar yield of syringic acid to 32.5%. However, this also led to a higher formation of syringol and the sodium salt of guaiacol due to the sodium–proton exchange mechanism between SyONa and guaiacol. The sodium salt subsequently underwent carboxylation, producing HBA products of guaiacol with a yield of 8.82% after 4 hours. Additionally, GC–MS analysis identified various syringol and guaiacol and their corresponding HBA derivatives as by-products, formed through methyl substitution and proton exchange reactions involving methoxy (–OCH<sub>3</sub>), hydroxyl (–OH), and carboxyl (COOH) groups.

In contrast, the use of K<sub>2</sub>CO<sub>3</sub> alongside SyONa promoted a more selective reaction pathway, yielding syringic acid with minimal by-products. Across varying CO<sub>2</sub> pressures (5, 10, 30, and 50 bar), K<sub>2</sub>CO<sub>3</sub> maintained syringic acid yields between 15.3% and 24.4%, while reducing the formation of side products such as methyl syringate and 1,2,3-TMB. Regarding reaction time, the maximum syringic acid yield of 39.2% was achieved at 6 hours with minimal by-products.

A mechanistic analysis was also proposed. In syringolate, both *ortho*-positions are blocked by methoxy groups, preventing the conventional *ortho*-carboxylation pathway established for phenol. Consequently, the unpromoted reaction proceeds through an intrinsically disfavoured *para*-carboxylation route. In the presence of K<sub>2</sub>CO<sub>3</sub>, the two carbonate oxyanions can interact simultaneously with the *para*-C–H bond, helping to pre-organise the ion pair and weaken the C–H bond so that carboxylation becomes more accessible. Guaiacol, in contrast, can interact with the *para*-C–H bond only through a single oxygen atom, providing much weaker activation; instead, it mainly undergoes sodium–proton exchange with SyONa, consistent with prior observations. These findings suggest that direct CO<sub>2</sub> insertion into syringol to form syringic acid is feasible, though the choice of promoter is crucial for improving efficiency. In addition, the results highlight a promising strategy for converting CO<sub>2</sub> into high-value aromatic acids, and future studies may further optimise conditions and explore biomass-derived syringol as a sustainable feedstock for scalable CO<sub>2</sub> utilisation.

## Author contributions

Omar Mohammad: investigation, methodology, data curation, validation, visualization, writing – original draft, and writing – review and editing. Jude A. Onwudili: conceptualization, funding acquisition, methodology, visualization, supervision, project administration, writing – original draft, and writing –

review & editing. Qingchun Yuan: supervision, project administration, visualisation, and writing – review & editing.

## Conflicts of interest

There are no conflicts to declare.

## Data availability

All data relating to this work have been included in this article.

Supplementary information (SI): the calibration curve for syringol in water–acetone (50% v/v) solution (Fig. S1) and GC/MS-derived normalised peak area data showing the effects of pressure and reaction time on product distribution in the solid and toluene fractions for reactions of the sodium salt of syringol (SyONa) with 50 wt% guaiacol or 50 wt% K<sub>2</sub>CO<sub>3</sub> (Tables S1–S4). See DOI: <https://doi.org/10.1039/d5su00232j>.

## Acknowledgements

The authors acknowledge financial support from the College of Engineering and Physical Sciences, Aston University, through the EPSRC Doctoral Training Centre, grant number EP/T518128/1 for PhD Studentship (Omar Mohammad). All technical support from the Energy and Bioproducts Research Institute (EBRI) is also gratefully acknowledged.

## References

- C. Srinivasulu, M. Ramgopal, G. Ramanjaneyulu, C. M. Anuradha and C. Suresh Kumar, Syringic acid (SA) – A Review of Its Occurrence, Biosynthesis, Pharmacological and Industrial Importance, *Biomed. Pharmacother.*, 2018, **108**, 547–557.
- R. Ikeda, H. Uyama and S. Kobayashi, Novel synthetic pathway to a poly(phenylene oxide). Laccase-catalyzed oxidative polymerization of syringic acid, *Macromolecules*, 1996, **29**, 3053–3054.
- N. Zhou, W. P. D. W. Thilakarathna, Q. S. He and H. P. V. Rupasinghe, A Review: Depolymerization of Lignin to Generate High-Value Bio-Products: Opportunities, Challenges, and Prospects, *Front. Energy Res.*, 2022, **9**, 758744.
- D. Huang and Z. Yu, A synthesis method of high-purity, high-yield syringic acid, Chinese invention patent application, CN104693022A, Shouguang Haoyuan Chemical Co., Ltd, 2015.
- Tate Intellectual Property Office of China, CN102649724A, 2012.
- X. Liu, Y. An and H. Gao, Engineering cascade biocatalysis in whole cells for syringic acid bioproduction, *Microb. Cell Fact.*, 2024, **23**, 162.
- Q. H. Zeng, H. Zhang and J. L. Lin, Method for preparing syringic acid, Chinese invention patent application, CN104193617A, Zunyi Normal University, 2014.



- 8 C. A. E. Costa, C. A. Vega-Aguilar and A. E. Rodrigues, Added-Value Chemicals from Lignin Oxidation, *Molecules*, 2021, **26**, 4602.
- 9 M. Herbaut, A. Zoghalmi, A. Habrant, X. Falourd, L. Foucat, B. Chabbert and G. Paës, Multimodal analysis of pretreated biomass species highlights generic markers of lignocellulose recalcitrance, *Biotechnol. Biofuels*, 2018, **11**, 52.
- 10 R. Schmitt, Beitrag zur Kenntniss der Kolbe'schen Salicylsäure Synthese, *J. Prakt. Chem.*, 1885, (31), 397–411.
- 11 O. Mohammad, J. A. Onwudili and Q. Yuan, A critical review of the production of hydroxyaromatic carboxylic acids as a sustainable method for chemical utilisation and fixation of CO<sub>2</sub>, *RSC Sustainability*, 2023, **1**, 404–417.
- 12 RC Market Analytics, *Syringic Acid Market Size, Trends & Growth Statistics Report to 2030*, <https://www.rcmarketanalytics.com/syringic-acid-market/>, accessed 22 January 2025.
- 13 S. Guenther, G. Chi, B. Bera, T. Mickle and S. Bera, Methylphenidate-prodrugs, processes of making and using the same, *EP Pat.*, EP3189840B1, Kempfarm, Inc., 2021.
- 14 S. Erickson, Y.-W. Feng, C. Galopin, S. Gravina, Y. Kurash, T. Lee, L. Nattress and T. Wang, Glucosyringic acid analogs as sweetness profile modifiers, *US Pat.*, US10966447B2, PepsiCo, Inc., 2021.
- 15 O. Mohammad, J. A. Onwudili, Q. Yuan and R. Evans, Optimisation of reaction temperature during carboxylation of single and mixed model bio-derived phenolics as effective route for CO<sub>2</sub> utilisation, *Carbon Capture Sci. Technol.*, 2025, **15**, 100442.
- 16 S. Marasse, Process of making salicylic acid, *US Pat.*, US529182A, 1894.
- 17 O. Mohammad, J. A. Onwudili, Q. Yuan and R. Evans, Effective Chemical Fixation of CO<sub>2</sub> into Phenol Using Conventional Gas-Solid and Novel Suspension-Based Kolbe-Schmitt Reactions, *ChemSusChem*, 2025, **18**, e202402564.
- 18 A. S. Lindsey and H. Jeskey, The Kolbe-Schmitt Reaction, *Chem. Rev.*, 1957, **57**, 583–620.
- 19 O. Mohammad, J. A. Onwudili and Q. Yuan, Potential Large-Scale CO<sub>2</sub> Utilisation for Salicylic Acid Production via a Suspension-Based Kolbe-Schmitt Reaction in Toluene, *Molecules*, 2024, **29**, 2527.
- 20 L. Feng, X. Li, Z. Wang and B. Liu, Catalytic hydrothermal liquefaction of lignin for production of aromatic hydrocarbon over metal supported mesoporous catalyst, *Bioresour. Technol.*, 2021, **323**, 124569.
- 21 O. Mohammad, J. A. Onwudili, Q. Yuan and R. Evans, Advancing CO<sub>2</sub> utilisation via suspension-based carboxylation of single and mixed biomass-derived phenolics to produce high-value hydroxybenzoic acids, *Chem. Eng. J.*, 2025, 163498.
- 22 H. Kolbe, Ueber Synthese der Salicylsäure, *Adv. Cycloaddit.*, 1860, **113**, 125–127.
- 23 Z. Marković, S. Marković, N. Manojlović and J. Predojević-Simović, Mechanism of the kolbe-schmitt reaction. structure of the intermediate potassium phenoxide-CO<sub>2</sub> complex, *J. Chem. Inf. Model.*, 2007, **47**, 1520–1525.
- 24 Z. Marković, J. P. Engelbrecht and S. Marković, Theoretical study of the Kolbe-Schmitt reaction mechanism, *Z. Naturforsch., A:Phys. Sci.*, 2002, **57**, 812–818.
- 25 Y. Kosugi, Y. Imaoka, F. Gotoh, M. A. Rahim, Y. Matsui and K. Sakanishi, Carboxylations of alkali metal phenoxides with carbon dioxide, *Org. Biomol. Chem.*, 2003, **1**, 817–821.
- 26 T. M. Porter and M. W. Kanan, Carbonate-promoted C-H carboxylation of electron-rich heteroarenes, *Chem. Sci.*, 2020, **11**, 11936–11944.
- 27 D. J. Xiao, E. D. Chant, A. D. Frankhouser, Y. Chen, A. Yau, N. M. Washton and M. W. Kanan, A closed cycle for esterifying aromatic hydrocarbons with CO<sub>2</sub> and alcohol, *Nat. Chem.*, 2019, **11**, 940–947.
- 28 M. A. Varfolomeev, D. I. Abaidullina, B. N. Solomonov, S. P. Verevkin and V. N. Emel'yanenko, Pairwise Substitution Effects, Inter- and Intramolecular Hydrogen Bonds in Methoxyphenols and Dimethoxybenzenes. Thermochemistry, Calorimetry, and First-Principles Calculations, *J. Phys. Chem. B*, 2010, **114**, 16503–16516.
- 29 S. J. Grabowski, Hydrogen bond types which do not fit accepted definitions, *Chem. Commun.*, 2024, **60**, 6239–6255.

